

## Comparative Study of 1.3 and 1.5 $\mu\text{m}$ Light-Emitting Diodes GaAs-Based InAs/InGaAs and InAs/(Ga, In) (N, As) Self-Assembled Quantum Dots

<sup>1</sup>O.A. Niasse, <sup>1</sup>B. Ba, <sup>1</sup>A. Ndiaye, <sup>1</sup>F. Mbaye, <sup>1</sup>A. Lo, <sup>2</sup>A. Bèye and <sup>3</sup>O. Tottereau

<sup>1</sup>Laboratoire des Semi-conducteurs et d'Energie Solaire, Faculté des Sciences et Techniques, Université Cheikh Anta Diop de Dakar, BP: 5005, Sénégal

<sup>2</sup>Groupe de Physique des Matériaux, Département de Physique, Faculté des Sciences et Techniques, Université Cheikh Anta Diop, BP: 5005, Dakar, Sénégal

<sup>3</sup>Centre de Recherche sur l'Hétéro-épitaxie et ses Applications du CNRS, 06560, Valbonne, France

**Abstract:** This study presents self-assembled quantum dots structures made on GaAs substrate. The samples were grown by Molecular Beam Epitaxy (MBE) in the Stranski-Krastanow (SK) growth mode. Two types of quantum dots structures are performed under different growth conditions and are compared: the first type is composed of two structures with InAs quantum dots encapsulated with (Ga, In) (N, As) and the second one with boxes wrapped with InGaAs. The influence of encapsulation of quantum dots is highlighted and as already shown, the redshift of emission wavelength depends on nitrogen doping. Further investigations are done through the incorporation of indium and nitrogen in the quantum dots structures in order to understand their optimal doping level on electrical and optical properties. The effects of temperature, an important growth parameter, are examined through images of nanostructures obtained by Atomic Force Microscopy (AFM) and Scanning Electronic Microscopy (SEM) techniques.

**Keywords:** Dislocations, epitaxy, Molecular Beam Epitaxy (MBE), photoluminescence, quantum dots, RHEED, Scanning Electronic Microscopy (SEM)

### INTRODUCTION

The realization of self-assembled quantum dots nanostructures in which the electron is confined in the three directions of space combined to the discretization of the electronic states, make these devices as ideal photon sources for applications in telecommunication, signal processing and material characterization (Gladyshev *et al.*, 2006; Sek *et al.*, 2007). This carriers confinement in space on dimensions comparable to their Broglie wavelength, confer interesting physical properties to these new types of Quantum Dots (QD) components as InAs/InGaAs and InAs/(Ga, In) (N, As) self-assembled quantum dots grown on GaAs substrate. It is used as quantum well laser diodes for optoelectronic devices and shows great promise in quantum dots, but the growth temperature is a limiting factor in the fabrication of the devices. The growth temperature of (Ga, In) (As, N) (450°C) is lower than that of GaAs (600°C). It is known that the optimum optical properties of nitrogen samples are obtained at 450°C while best transport properties for GaAs occur at 600°C. Consequently, a compromise must be found for

applications related to transport properties at low temperature suitable to the growth of (Ga, In) (As, N) and high temperature needed for the growth in the GaAs matrix. Otherwise the creation of high densities of defects related to excess of arsenic will affect the structural and optical properties of the structures. The annealing allows reducing these defects in order to lower the laser threshold current of quantum dots. The quality of the samples made is examined through optical and electrical characterization from Photoluminescence (PL) spectra, Electroluminescence (EL) spectra and courant-Voltage I(V) characteristics. The threshold current obtained with structures encapsulated with GINA are compared with those already obtained and capped with InGaAs Kobayashi *et al.* (1996). A significant shift in wavelength toward the red and low threshold currents are examined through the influence of capping layers.

In this study, the aim is to realize GaAs based nanometer-sized semiconductors quantum dots emitting in wavelength range 1.3 to 1.5  $\mu\text{m}$ . From theoretical considerations, the quaternary (Ga, In) (As, N) seems to be suitable for such applications, in the sense that it

Table 1: Thickness and doping layer of a GINA laser QD

Layer type	Material and composition	Thickness (nm)	Doping ( $\times 10^{18}/\text{cm}^3$ )
Barrier	GaAs	200	Doped (Be) p+
	$\text{Al}_{0.35}\text{Ga}_{0.65}\text{As}$	1000	Doped (Be) p
	$\text{Al}_{0.35}\text{Ga}_{0.65}\text{As}$	300	Undoped
	GaAs	120	Undoped
Active layer	$\text{Ga}_{1-x}\text{In}_x\text{N}_y\text{As}_{1-y}$		
	InAs		
	InGaAs		
Barrier	GaAs	120	Nid
p-cladding2	$\text{Al}_{0.35}\text{Ga}_{0.65}\text{As}$	300	1 to 3.4 (Si)
p-cladding	$\text{Al}_{0.35}\text{Ga}_{0.65}\text{As}$	1000	3.4 (Si)
Buffer 1	GaAs	200	5 (Si)
Substrate (n)	GaAs	350000	

allows to overcome some constraints of dislocation that create non-radiative recombination in the laser structure.

The influence of the MBE growth conditions (substrate temperature, pressure, surface reconstruction of the subsequent layers) on the optical properties of the self-assembled InAs/GaAs quantum dots is investigated. The ternary and quaternary (Ga, In) (N, As) buffer and/or capping layers are used to optimize the quality of the heterostructure for instance preventing inter-impurity diffusion or carrier screening by parent impurities and increasing the gain in density carrier in the active region.

The growth conditions which determine the quality of the resulting structure are optimized to realize quantum dots emitting either at 1.3 or at 1.5  $\mu\text{m}$ . The emission energy and line-width and the separation between ground and excited states are measured using photoluminescence spectroscopy.

**Experimental procedure:** The samples studied in this study were grown by Molecular Beam Epitaxy (MBE) technique, which is a vacuum evaporation of atoms or molecules placed on sources in effusion cells. The growth of the different layers of optoelectronic devices was made using a Riber 32 MBE system with Ga, Al, In and As solid sources and a nitrogen gas source. Two types of laser structures were fabricated using the parameters reported in Table 1 and relative to the targeted layer thicknesses and doping layer for a device made with InAs quantum dots encapsulated with (Ga, In) (N, As). The materials are deposited on a heated monocrystalline substrate where they diffuse and form a crystalline structure identical to that of the substrate.

The substrate is a single crystal GaAs (001) with a thickness of 350  $\mu\text{m}$ , a carrier density of about  $2.3 \times 10^{18}/\text{cm}^3$ . For the present study, growth duration and the corresponding temperature during the realization of the different layers are schematically drawn in Fig. 1.

After an initial oxide removal of GaAs substrate under arsenic flux at 600°C, a 200 nm-thick GaAs

buffer layer is grown on the GaAs substrate. The temperature is increased to 700°C, a 1  $\mu\text{m}$ -layer of AlGaAs is grown followed by a deposition of a 300 nm-thick layer of AlGaAs. Then the arsenic valve is closed in the As-rich (4×4) surface reconstruction. A Ga-rich (2×4) surface reconstruction is obtained by deposition of Ga to an equivalent of 1, 7 Monolayer (ML) GaAs at 400°C after closing the arsenic valve. A layer of indium is then deposited to an equivalent of 2 and 12 ML InAs after the As background pressure is below to  $2.10^{-9}$  torr. On both sides of the active zone, there are two layers of AlGaAs: the lower layer is doped with silicon, the upper one is p-doped beryllium. A 120 nm-layer of GaAs not intentionally doped (nid) is inserted between the doped AlGaAs layers and the active area. The AlGaAs layers are highly doped and their association with GaAs minimizes losses by free carrier absorption in the InAs active zone between the Bragg mirrors AlGaAs/GaAs. To prevent a possible diffusion of beryllium atoms in the GaAs cavity, a 300 nm layer of AlGaAs (nest) is inserted between the cavity and the thickest p-type AlGaAs. Consequently, the optical cavity, formed by the cleavage facets in the plane and by the refractive index variation along the growth direction, can confine photons in the active zone. A heavy doping is used for the ohmic contact layers which are deposited by electronic evaporation or by Joule effect after etching by photolithography. These contacts allow performing electrical measurements that provide information on the sensitivity, the stability and the power consumption heating of the structure built.

In this study, four quantum dots structures are fabricated, two of them, capped with InGaAs, are referred as samples S997 and S1005, the two others with boxes wrapped in GINA, are named S1008 and S1009. The S997, S1008 and S1009 samples are made with five series of boxes plans to increase the gain in density carriers in the active region, whereas the S1005 is performed with only one series of boxes. The incorporation rate of nitrogen in samples capped with GINA is about 1% for S1008 and 1.8% for S1009, the composition of indium is 15 and 20% respectively. For samples S1005 and S1008, the InAs self-assembled QD layer are capped with a 5 nm-thick  $\text{Ga}_{1-x}\text{In}_x\text{N}_{yy}\text{As}_{1-y}$  layer followed by a 5 nm-thick GaAs growth at 430°C. At the end, a 120 nm-thick GaAs layer is deposited at 580°C at a rate of 1MC/s. It should be noted that the annealing at 580°C made before to the deposition of InAs, allows to smooth the surface on which boxes will be formed and thus to improve the quality of these boxes. The goal is to minimize the threshold current in order to improve efficiency. For that, one of the two following solutions can be chosen: the first one is to

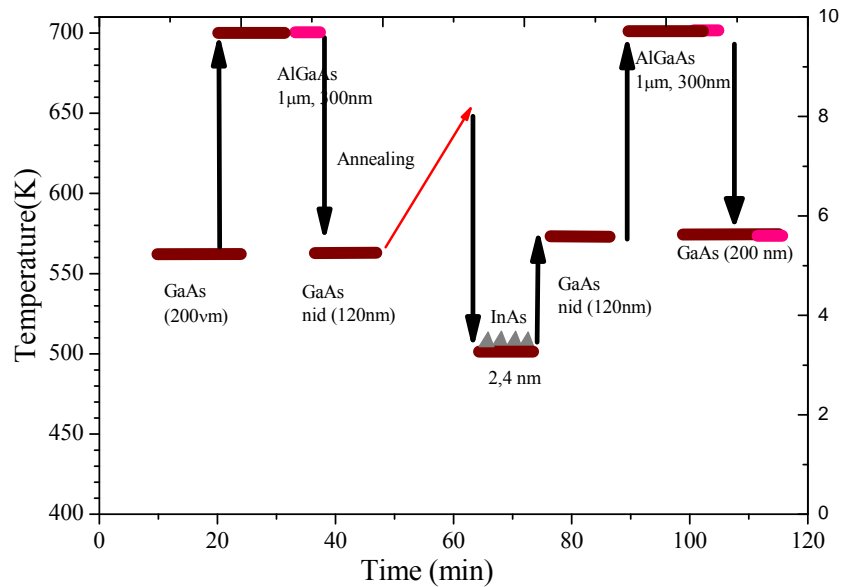


Fig. 1: The temperature cycle in the development of a laser structure based GINA quantum

contain the current over a small section; the second one is to confine photons in a small volume. The evolution of the surface morphology is studied *in situ* by Reflection High Energy Electron Diffraction (RHEED). Information on the morphology (size, density) of QDs is obtained after a direct analyze of data. The measurements of QDs size were performed *ex situ* by Atomic Force Microscopy (AFM) and Scanning Electronic Microscopy (SEM) techniques. The Photoluminescence (PL) measurements were realized at low temperature (10 K) using the 514 nm line of an Ar<sup>+</sup> laser and a liquid nitrogen cooled germanium detector. The samples were mounted p-side up on a closed helium cycle cryostat which allows cooling down to 14 K. The collected light from the devices was dispersed by a 1 m long monochromator and detected with a cooled germanium detector. The structure was tested under pulsed conditions, pulse widths being between 1 and 20  $\mu\text{m}$  and 1 to 10% duty cycles.

## RESULTS AND DISCUSSION

Figure 2 shows the AFM image of 3D InAs islands on GaAs of a sample S1042 grown following the same procedure than our four samples. This sample was not encapsulated in order to have, through its structural analysis, information about the morphology of our samples.

The AFM image shows boxes with pyramidal shape of a 6.5 nm average height for small boxes and 15 nm for larger boxes. To better visualize the

pyramidal shape in 3D, the scale 1 division for 30 nm along the z axis and 1 division for 0.2  $\mu\text{m}$  along the x axis is chosen. The AFM image allows identifying three types of quantum dots: small, medium and large. The density of QDs obtained for the sample S1024 is  $3.8 \times 10^{10} \text{ cm}^{-2}$ . The big boxes are formed by coalescence called "islands coalesced". They induce dislocations particularly when the quantum dots are subsequently covered with a layer of GINA during encapsulation. These dislocations act as non radiative recombination centers and strongly affect the luminescence of quantum dots. Therefore the density of these islands coalesced must be minimized as much as possible to avoid nonradioactive recombination due to these types of defects. The inhomogeneity in patch size is observed in SEM as shown in Fig. 3. The measurements were made using the voltage of 10 kV on a scale of 20 nm. The sample shows a rather different morphology with various size and density of the QD which can be explained by the fluctuation of temperature in the growth room. The hetero-epitaxial quantum dot not support change in temperature during the deposition of the different layers; this affects the quality of the boxes as also a number of other critical issues such as the influence of arsenic pressure, substrate temperature and growth procedure with or without growth interruption during InAs deposition in the formation of these 3D InAs quantum dots islands (Gladyshev *et al.*, 2006; Sek *et al.*, 2007).

Figure 4 shows the Photoluminescence (PL) spectra at 10 K for our four samples made in GaAs

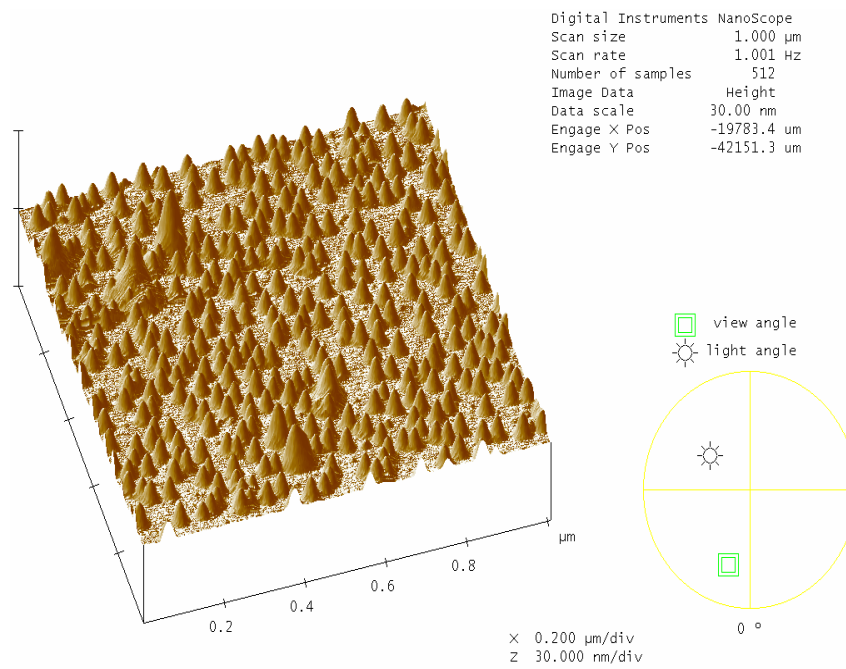


Fig. 2: AFM images of 3D InAs islands on GaAs in sample S1024

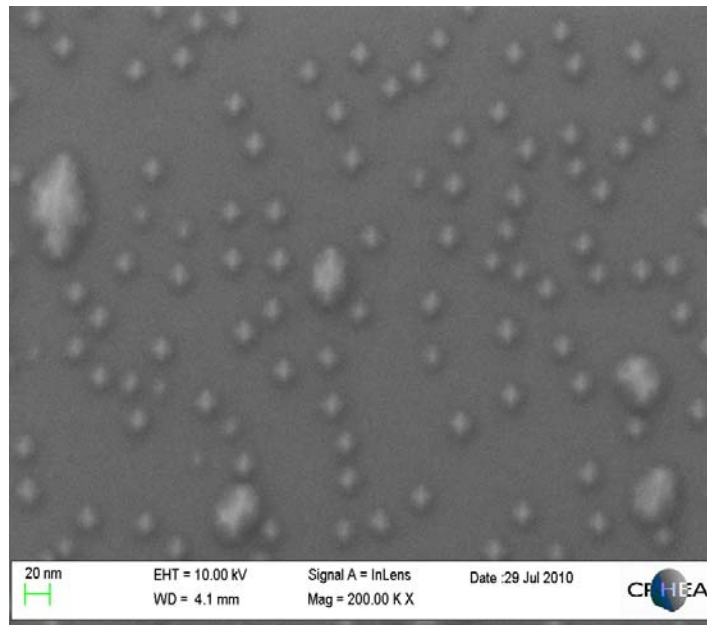


Fig. 3: SEM images of quantum dots for sample S1024

matrix PL spectra shows the emission wavelength of the samples after an optical excitation with an intensity of 10 mW. For the QD structures, it is noted that the shift of the maximum PL intensity towards the longer wavelengths is accompanied with a reduction of the amplitude. For the different samples, energy emissions are observed at 0.985 eV (S997), 1.035 eV (S1005),

0.950 eV (S1008) and 0.900 eV (S1009). The result obtained by fitting in the PL spectre is reported in the Table 2. These energies correspond to the fundamental transition resulting from the recombination between an electron located at the lowest energy of conduction band in the active zone (InAs/InGaAs) and a hole located in the upper level of the valence band. Table 2

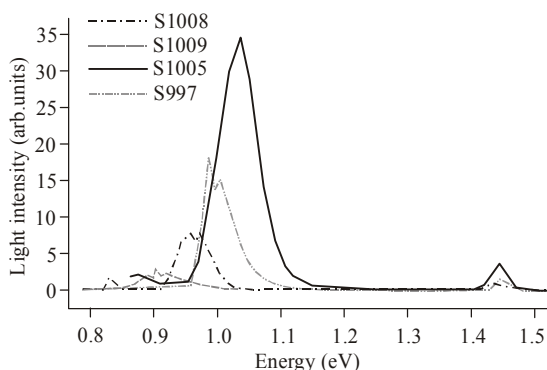


Fig. 4: PL spectra of four structures InAs/GaAs structures with different capping layers at 10 K with an excitation intensity of 10 mW

Table 2: Summary of results obtained in photoluminescence at 10 K

Samples	Type	Series	Fundamental	FWHM
InGaAs	S	5	1265 nm	55
		1	1198 nm	80
GINA	S	5	1305 nm	68
		5	1377 nm	97

outlines the peak wavelength of these transitions for each sample with the associated values of the Full Width at Half Maximum (FWHM).

It is clearly observed that the sample S1005 presents the strongest peak intensity at wavelength 1.198  $\mu\text{m}$  whereas it is 1.265  $\mu\text{m}$  for the sample S997: the increase in wavelength and the decrease in PL intensity for these two structures with InGaAs encapsulation can be explained by the increase in the number of series of boxes (one series of boxes for S1005 and five series for S997). The sample S997 presents a smaller FWHM (55 meV) compared to that of QD structures as S1008, S1009 and S1005. This smaller value can be linked to the increase of number of series boxes and shows that the sample S997 presents the best laser results. Samples with structures GaAs-based InAs/GINA give longer wavelengths compared to that for samples GaAs-based InAs/InGaAs as shown in Table 2.

For all samples, a transition appears at 1.46 eV and corresponds to the transition in the GaAs layer. It can also be noticed in Fig. 4, for samples S1008 and S1009, that the incorporation of nitrogen results in a decrease in the PL intensity of the devices and a wavelength shift to the red as outlined in Hugues *et al.* (year) show also that the introduction of nitrogen in the growth modifies the diffusion length of atoms and leads to a decrease in the density of QD and especially to an increase in the homogeneity of their size so the FWHM of the samples are increased. The wavelength emission of the sample S1009, with a higher rate of 2% Nitrogen and about 15

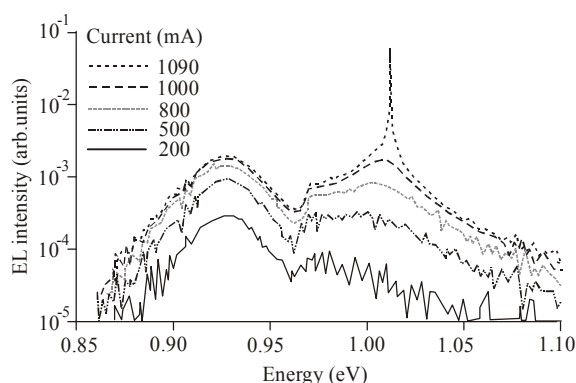


Fig. 5: E.L Spectra of S997 at room temperature under pulsed conditions with different electrical excitations (1 KHz, 480 A/cm<sup>2</sup>)

to 20% indium shifts toward the red with a sharp drop in light output and a greater FWHM (97 nm). This power loss is associated with a significant concentration of defects induced by nitrogen that has low miscibility with the alloy (Ga, In). The concentration of indium is in turn limited by the compressive stress it generates. A heat treatment can eliminate the defects that could be induced by nitrogen as mentioned in studies (Songmuang *et al.*, 2003; Montes *et al.*, 2009) showing that the samples annealed at high temperature  $T \geq 850^\circ\text{C}$  yield a better quality QD nanostructures with a significant increase in the intensity emitted. For a good optimization, the concentration of nitrogen should be minimal to limit the drop in the radiative efficiency and the inhomogeneous broadening of the photoluminescence spectra. Studies for optimization of these parameters are performed in works which show that: an increase in growth temperature causes an increase in QD size, a decrease in density and improve uniformity in size (Sek *et al.*, 2007), a decrease in the deposition rate results in a decreased density and higher dimensions (Songmuang *et al.*, 2003) which show that increasing the amount deposited causes an increase in density until saturation and improves size distribution Kobayashi *et al.* (1996).

Information on the evolution of the growth parameters were confirmed after analysis of nanostructures with quantum dots laser realized.

Figure 5 shows the Electroluminescence (EL) spectra of best laser structure (sample S997) performed for different electrical excitations.

For an electrical stimulus of 200 mA, only one peak is observed at 0.92 eV. By increasing the excitation intensity from 500 mA up to higher values, it is observed the apparition of a shoulder at 1.005 eV which become more intense as the excitation is increased. For an 1000 mA excitation intensity, an EL

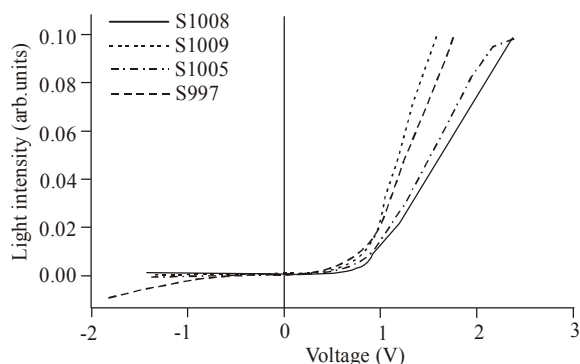


Fig. 6: Current-voltage characteristic of the four QD structures

Table 3: Threshold voltage

Samples	Threshold voltage (V)	Threshold current (mA)
S997	0.54	77.34
S1005	0.52	54.37
S1009	0.54	94.26
S1008	0.50	55.09

peak intensity appears at 1.011 eV. By increasing the excitation to 1090 mA excitation, the structure lases at 1.26  $\mu\text{m}$ . This peak corresponds to the excited state and the first peak in the ground state. So our quantum dot structure, lasing ground state upholding an emission wavelength of 1.34  $\mu\text{m}$  and with the containment barrier and the effect of the encapsulation layer might have reached a wavelength of issue of 1.55  $\mu\text{m}$ . The gap between the ground state energy (0.95 eV) and the first excited state (1.011 eV) is 84 meV and a similar gap is obtained by Hospodkova *et al.* (2011).

The current-voltage characteristics of the sample S997 are illustrated on Fig. 6. Well for one, we chose to measure the two lengths of ribbon 430 microns and 440 microns and the curves are shown in Fig. 6.

The current-voltage characteristic of a quantum dot laser structure has the same gain as the p-n junction.

These important characteristics are:

- The average forward current it can bear constantly in our measurements we did not exceed 0.1 A for example
- The direct current that can withstand peak pulsed
- The maximum reverse voltage  $V_{Rmax}$  permissible without damage

The threshold voltages obtained for our samples are summarized in Table 3.

We find that most of our structures have almost the same threshold voltage but the boxes are smaller than the threshold voltage of the quantum well structure.

The equivalent circuit model for a simplified case can be represented by a threshold and a dynamic resistance but in the real case, the model would be more complex because there would be significant capacitive effects which are due to the composition of the charge region space. So for a bias voltage below the threshold current ( $V_D < V_0$ ), the diode behaves like a closed switch. For  $V_D > V_0$ , the diode conduction causes a voltage drop equal to  $V_D = V_0 + V_0 R_D I$ . It is possible to deduce from these curves the dynamic resistance. It is given by the slope of the linear part of the curve; the calculated value is  $\sim 10\Omega$ . Structures for quantum dot laser, the same value of threshold voltage is denoted by cons for the quantum well structure, in two widths of tape, there is a difference in threshold voltage of the same sample. This highlights the influence of the length of the ribbon on the electrical characteristics already observed in measurements of light output as a function of excitation intensity  $P(I)$ .

## CONCLUSION

The study of optical and electrical properties reveals that draws more and more towards red. For this, there is a low light intensity and a broadening of the FWHM nanostructures GINA. This reflects a poor quality of the quantum dot structure caused by the presence of defects associated with dislocation and coalescence of islands. The current study was focused on increasing the density of quantum dots but the main problem is the growth temperature of laser structures GINA to make optoelectronic devices. The epitaxial layers should overlap without many constraints (e.g., GaAs, InGaAs) have different temperature gradients and are very sensitive to variation thereof. At that point defects (dislocations and coalescence of islands) in the case of quantum dot structures are not conducive to the formation of a good laser structure. Thus the challenge of controlling the growth temperature structures GINA specially those boxes is far from won and the field of exploration that remains relevant today.

## ACKNOWLEDGMENT

This study was supported by the Office of International Cooperation of the University Cheikh Anta Diop, Dakar (Senegal) and the CNRS (France).

## REFERENCES

- Gladyshev, A.G., N.V. Kryzhanovskaya, A.M. Nadtochy, E.S. Semenova, A.E. Zhukov, A.P. Vasil'ev, V.S. Mikhrin, Y.G. Musikhin, M.V. Maximov, N.N. Ledentsov and V.M. Ustinov, 2006. Comparative study of GaAs-based 1, 5 micron-range InAs/InGaAlAs self-assembled quantum dots. Phys. Status Solidi. A, 203(6): 1359.

- Hospodkova, A.P., J. Oswald, J. Hazdra and P. Kuldova, 2011. Influence of strain reducing layers on electroluminescence and photoluminescence of InAs/GaAs QD structures. *J. Crystal Growth*, 315(1): 110-113.
- Hughes, J.B., G.C. Daily and P.R. Ehrlich, 1997. Population diversity: Its extent and extinction. *Science*, 278: 689-692.
- Kobayashi, N.P., T.R. Ramachandran, P. Chen and A. Madhukar, 1996. In situ, atomic force microscope studies of the evolution of InAs three-dimensional islands on GaAs (001). *Appl. Phys. Lett.*, 68: 3299.
- Montes, M., A. Hierro, J.M. Ulloa, A. Guzmán, M. Al Khalfioui, M. Hugues, B. Damilano and J. Massies, 2009. Electroluminescences analysis of 1.3-1.5 $\mu$ m InAs quantum dots LEDs with (Ga,In)(N,As) capping layers. *Phys. Status Solidi C*, 6: 1424.
- Sek, G., K. Ryczko, M. Molyka, J. Andrzejewski, K. Wysocka, J. Misiewicz, L.H. Li, A. Fione and G. Patriarche, 2007. Effect of intermixing and capping layer. *J. Appl. Phys.*, 101: 063539.
- Songmuang, R., S. Kiravittaya, M. Sawadsaringkan, S. Panyakeow and O.G. Schmidt, 2003. Photoluminescence investigation of low-temperature capped self-assembled InAs/GaAs quantum dots. *J. Cryst. Growth*, 251: 166-171.